remote sensing

MDPI

Article

Monitoring and Predicting Drought Based on Multiple Indicators in an Arid Area, China

Yunqian Wang [1,2,3,4], Jing Yang [5,*], Yaning Chen [2], Zhicheng Su [6], Baofu Li [1], Hao Guo [1] and Philippe De Maeyer [3,7]

1 School of Geography and Tourism, Qufu Normal University, Rizhao 276826, China; wangyq@qfnu.edu.cn (Y.W.); libf@qfnu.edu.cn (B.L.); guohao@qfnu.edu.cn (H.G.)
2 State Key Laboratory of Desert and Oasis Ecology, Xinjiang Institute of Ecology and Geography, Chinese Academy of Sciences, Urumqi 830011, China; chenyn@ms.xjb.ac.cn
3 Department of Geography, Ghent University, 9000 Ghent, Belgium; Philippe.DeMaeyer@UGent.be
4 Sino-Belgian Joint Laboratory of Geo-information, Urumqi 830011, China
5 National Institute of Water and Atmospheric Research, Christchurch 8000, New Zealand
6 China Institute of Water Resources and Hydropower Research, Beijing 100038, China; suzhc@iwhr.com
7 Sino-Belgian Joint Laboratory of Geo-information, 9000 Ghent, Belgium
* Correspondence: jing.yang@niwa.co.nz

Received: 1 June 2020; Accepted: 15 July 2020; Published: 17 July 2020

Abstract: Droughts are one of the costliest natural disasters. Reliable drought monitoring and prediction are valuable for drought relief management. This study monitors and predicts droughts in Xinjiang, an arid area in China, based on the three drought indicators, i.e., the Standardized Precipitation Index (SPI), the Standardized Soil Moisture Index (SSMI) and the Multivariate Standardized Drought Index (MSDI). Results indicate that although these three indicators could capture severe historical drought events in the study area, the spatial coverage, persistence and severity of the droughts would vary regarding different indicators. The MSDI could best describe the overall drought conditions by incorporating the characteristics of the SPI and SSMI. For the drought prediction, the predictive skill of all indicators gradually decayed with the increasing lead time. Specifically, the SPI only showed the predictive skill at a 1-month lead time, the MSDI performed best in capturing droughts at 1- to 2-month lead times and the SSMI was accurate up to a 3-month lead time owing to its high persistence. These findings might provide scientific support for the local drought management.

Keywords: drought monitoring; drought prediction; multiple drought indicators; soil moisture; precipitation; arid

1. Introduction

Droughts are one of the costliest natural disasters and have seriously destructive effects on the ecological environment, agricultural production and socio-economic conditions [1]. According to a recent report from the Food and Agriculture Organization of the United Nations (FAO), droughts were responsible for agricultural losses at a total of USD 29 billion in the developing countries between 2005 and 2015 [2]. Most parts of the world experience droughts, especially in the arid regions where the annual rainfall mainly derives from a few rainfall events [3]. Recent studies report that the drought frequency and intensity may increase under global warming [4,5], thus it is vital to establish reliable drought monitoring and early warning systems to assist the decision-makers in coping with these disasters.

Since droughts affect a wide variety of sectors, it is difficult to define the droughts uniquely [6]. Typically, droughts can be divided into meteorological droughts related to precipitation, agricultural

drought related to soil moisture and hydrological drought related to runoff [7]. Accordingly, both multivariate and univariate drought indices have been developed to monitor different aspects of droughts. For example, the Standardized Precipitation Index (SPI), developed by Mckee et al. (1993) [8], has been widely used to monitor the meteorological drought. The SPI is calculated by fitting and transforming the long-term record of precipitation to a normal distribution. The strength of the SPI is that it can be calculated across various timescales (e.g., 3-, 6-, 9- and 12-month). According to the concept of the SPI, the Standardized Soil Moisture Index (SSMI) and Standardized Runoff Index (SRI) are proposed so as to monitor the agricultural and hydrological droughts, respectively [9,10]. Multivariate drought indicators have also been developed to characterize more drought features, which include the Standardized Precipitation Evapotranspiration Index (SPEI) [11], the Optimal Blended NLDAS (North American Land Data Assimilation System) Drought Index (OBNDI) [12], the Multivariate Standardized Drought Index (MSDI) [13] and so on. The performance differs for these drought indicators. For example, previous studies suggest that a precipitation index is suitable to monitor the drought onset, while a soil moisture index proves better in detecting the drought persistence and the integration of the soil moisture and precipitation may be more efficient for the drought monitoring [14–16].

In addition, various drought prediction methods have been developed, based on either statistical or dynamical methods [17,18]. The statistical methods, such as the regression models, probability distribution methods, artificial intelligence methods and Ensemble Streamflow Prediction (ESP), generally rely on the empirical relations of historical data [19,20], while the dynamical methods, such as the North American Multi-Model Ensemble (NMME), General Circulation Models (GCMs) and hydrological models are generally based on the simulation of the physical processes of the atmosphere, ocean and land surface [21,22]. Both the statistical and dynamical methods have their advantages and disadvantages. The statistical methods are simple to implement and useful to provide base skill levels [23]. However, if the climate changes are not sufficiently captured from the historical records, the statistical methods may offer a low predictive skill [24]. The dynamical methods are adept at incorporating the non-stationarity aspects of the climate and predicting the unprecedented conditions [25], but they also tend to be time-consuming and fall prey to model errors and uncertainty [26]. Given these drawbacks, it is difficult to estimate which prediction method is the best. In fact, the selection of the most appropriate method may depend on the region, drought indicators, lead time and other factors [27].

The Xinjiang Uygur Autonomous Region is an arid region in Northwest China with scarce water resources and a fragile ecosystem. Drought is one of the major, natural recurring disasters in Xinjiang and it seriously threatens the local ecological environment, agricultural production and even human lives. Previous studies show that, under climate change, weather extremes (i.e., precipitation and temperature) are occurring more frequently in the region, which may increase the uncertainty of the drought occurrence [28,29]. However, to the best of our knowledge, there is no research yet on drought predictions for this region and only a few studies have monitored droughts based on a univariate index (i.e., the SPI) [30–32]. Hence, in this study, we used the Standardized Precipitation Index (SPI), Standardized Soil Moisture Index (SSMI) and Multivariate Standardized Drought Index (MSDI) (which integrates precipitation with soil moisture) to monitor and predict droughts in Xinjiang, China. When the dynamical methods are applied to predict the soil moisture, precipitation and temperature forecasts from dynamic models, or statistical methods, are generally used as input data to force the land surface or hydrologic models. In this case, both the input uncertainty and model errors are propagated into the soil moisture simulations, which may increase the uncertainty of the dynamic soil moisture forecasts [33,34]. Furthermore, previous studies also indicated that the dynamic methods offer high uncertainty and relatively low seasonal predictive skills [35,36]. For these reasons, the Ensemble Streamflow Prediction (ESP) method, widely applied in numerous climate and hydrological studies, is applied for the drought prediction in this study.

In the present study, we monitored and predicted droughts in Xinjiang based on three drought indicators (i.e., the SPI, SSMI and MSDI), which fill the gap of the drought research in the study area. The main aims of this study are: (1) to compare the different drought indicators (SPI, SSMI and MSDI) of drought monitoring by analyzing the spatial extent, severity and persistence of drought; (2) to predict the probability of drought occurrence using the ESP method based on three different drought indicators; finally, (3) to evaluate and compare the predictive skills based on multiple drought indicators with different lead times. The results of this study might help decision-makers to take effective measures in order to reduce the impact of drought.

2. Study Area and Data

2.1. Study Area

The Xinjiang Uygur Autonomous Region (34°15′–49°10′ N, 73°20′–96°25′ E) is located in the northwest of China (Figure 1). It exhibits a distinct style of basin-mountain topography with three mountain ranges (Altay Mountains, Tianshan Mountains and Kunlun Mountains) and two basins (Junggar Basin and Tarim Basin). The Tianshan Mountains divide Xinjiang into North and South Xinjiang. Xinjiang is located far from the sea and is surrounded by mountains, which results in a semi-arid and arid climate across the region [37,38] or a cold semi-arid (BSk) and cold desert (BWk) in the Köppen–Geiger climate classification [39]. The average annual precipitation of this region amounts to less than 150 mm scattered across an average of 55 days [31], while the annual potential evapotranspiration could reach 3000 mm in South Xinjiang [40]. The annual regional precipitation has a wide range, with 100–500 mm in North Xinjiang and less than 100 mm in South Xinjiang [41]. Overall, Xinjiang is characterized by scarce water resources and drought is one of the main obstacles to its economic and social development.

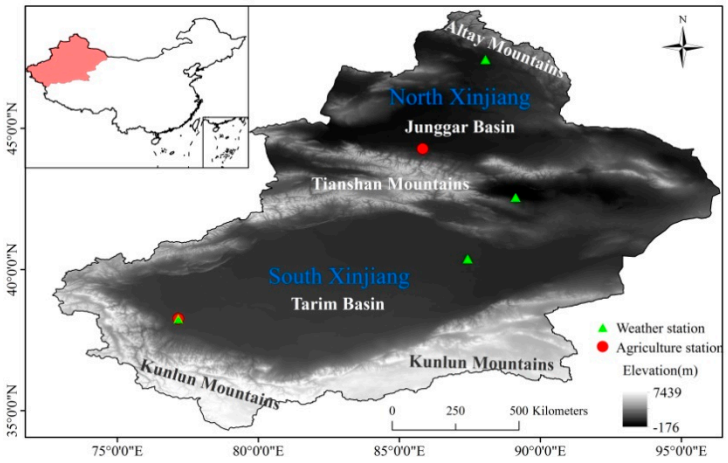

Figure 1. Geographical location of the study area.

2.2. Data

2.2.1. MERRA-Land Data

Modern-Era Retrospective analysis for Research and Applications (MERRA) provide long-term, global estimates of the precipitation and soil moisture through assimilating the in situ and remote sensing data. The MERRA-Land dataset is an improved product of the original MERRA dataset in land modeling [42]. The MERRA-Land data product is available at a spatial resolution of 0.5° × 0.667° from January 1980 to the present. In this study, the monthly data of the precipitation and topsoil layer (0–2 cm) soil moisture from MERRA-Land are applied to calculate the 6-month drought indicators (i.e., the SPI, SSMI and MSDI) for the drought monitoring and prediction.

2.2.2. In Situ Data

In this study, the in situ observations are employed to validate the MERRA-Land data. The in situ soil moisture and precipitation data are collected from two agriculture stations and four weather stations (Figure 1).

The Wulawusu station (44°28′ N, 85°82′ E), located in North Xinjiang, provides soil moisture data from 1982 to 1994. The Shache station (38°71′ N, 77°45′ E), located in South Xinjiang, provides the soil moisture data from 1990 to 2010. The soil moisture observations are measured three times a month at different depths (10 cm, 20 cm, 50 cm, 70 cm and 100 cm). Here, the monthly averaged soil moisture observations at the top layer (0–10 cm) are utilized.

Furthermore, the observed precipitation data from the Aletai (47°44′ N, 88°05′ E), Tulufan (42°56′ N, 89°12′ E), Tieganlike (40°38′ N, 87°42′ E) and Shache (38°71′ N, 77°45′ E) stations are applied so as to validate the MERRA-Land precipitation data. The data are provided by the Chinese meteorological station network on a monthly scale.

3. Methods

3.1. Calculation of the Drought Index

The 6-month SPI, SSMI and MSDI were calculated in the following steps. Firstly, the 6-month cumulative precipitation ($CP_{n,i}$) and soil moisture ($CSM_{n,i}$) for month i of year n are derived as:

$$CP_{n,i} = P_{n,i} + P_{n,i-1} + P_{n,i-2} + P_{n,i-3} + P_{n,i-4} + P_{n,i-5} \quad (1)$$

$$CSM_{n,i} = SM_{n,i} + SM_{n,i-1} + SM_{n,i-2} + SM_{n,i-3} + SM_{n,i-4} + SM_{n,i-5} \quad (2)$$

where $P_{n,i}$ and $SM_{n,i}$ represent the precipitation and soil moisture in month i of year n, respectively. Next, the empirical Gringorten plotting position formula [43] is applied to calculate the cumulative precipitation probabilities' distribution (p_P), soil moisture probabilities' distribution (p_{SM}) and joint probability distribution ($p_{(P,SM)}$), respectively:

$$p_P = \frac{k_P - 0.44}{n + 0.12} \quad (3)$$

$$p_{SM} = \frac{k_{SM} - 0.44}{n + 0.12} \quad (4)$$

$$p_{(P,SM)} = \frac{k_{(P,SM)} - 0.44}{n + 0.12} \quad (5)$$

where k_P denotes the rank of the cumulative precipitation, k_{SM} indicates the rank of the cumulative soil moisture, $k_{(P,SM)}$ refers to the number of data pairs (CP_i, CSM_i) for $CP_i \le CP$ and $CSM_i \le CSM$ ($1 \le i \le n$) and n shows the number of the observation. Finally, the *SPI*, *SSMI* and *MSDI* could be derived by standardizing the empirical probabilities as:

$$SPI = \varphi^{-1}(p_P) \quad (6)$$

$$SSMI = \varphi^{-1}(p_{SM}) \quad (7)$$

$$MSDI = \varphi^{-1}\left(p_{(P,SM)}\right) \quad (8)$$

where φ stands for the standard normal distribution function.

The drought classification used in this study is based on the U.S. Drought Monitor [44], as shown in Table 1. The negative drought index indicates a relatively dry condition, while the positive value illustrates a wet condition. There are five drought categories, while this study mainly concentrates on the drought conditions below D1 (threshold < −0.8).

Table 1. Classification of the drought severity.

Drought Index	Level	Description
≥2.0	W4	Exceptional wetness
[1.60, 1.99]	W3	Extreme wetness
[1.30, 1.59]	W2	Severe wetness
[0.80, 1.29]	W1	Moderate wetness
[0.50, 0.79]	W0	Abnormally wet
[−0.49, 0.49]	Normal	Normal
[−0.50, −0.79]	D0	Abnormally dry
[−0.80, −1.29]	D1	Moderate drought
[−1.30, −1.59]	D2	Severe drought
[−1.60, −1.99]	D3	Extreme drought
≤−2.0	D4	Exceptional drought

3.2. Drought Prediction

The Ensemble Streamflow Prediction (ESP) method [45,46], which assumes that historical records will possibly occur in the future, is employed to predict the occurrence probability of droughts based on the 6-month SPI, SSMI and MSDI. By assuming that the monthly precipitation and soil moisture data are available from the first year to year n, the drought prediction for the target month i of year n at a 1-month lead time could be derived based on the following processes. Firstly, the $n-1$ blended sequences of the 6-month cumulative precipitation ($CP^j_{n,i}$) and soil moisture ($CSM^j_{n,i}$) are derived as:

$$CP^j_{n,i} = P_{j,i} + P_{n,i-1} + P_{n,i-2} + P_{n,i-3} + P_{n,i-4} + P_{n,i-5}, \qquad j = 1,\ 2,\ 3, \ldots,\ n-1 \tag{9}$$

$$CSM^j_{n,i} = SM_{j,i} + SM_{n,i-1} + SM_{n,i-2} + SM_{n,i-3} + SM_{n,i-4} + SM_{n,i-5},\ j = 1,\ 2,\ 3, \ldots,\ n-1 \tag{10}$$

where ($P_{n,i-1}$, …, $P_{n,i-5}$) and ($SM_{n,i-1}$, …, $SM_{n,i-5}$) demonstrate the initial precipitation and soil moisture before the target month i of year n, and $P_{j,i}$ and $SM_{j,i}$ denote the historical precipitation and soil moisture records. For each blended cumulative precipitation $CP^j_{n,i}$ (j = 1, 2, … , $n-1$) and soil moisture $CSM^j_{n,i}$ (j = 1, 2, … , $n-1$), the corresponding SPI^j and $SSMI^j$ could be obtained based on the cumulative precipitation ($CP_{1,i}, \ldots, CP_{n-1,i}, CP^j_{n,i}$) and soil moisture ($CSM_{1,i}, \ldots, CSM_{n-1,i}, CSM^j_{n,i}$) from the historical records. The $MSDI^j$ might be calculated as:

$$MSDI^j = \varphi^{-1}\left[p\left(CP \le CP^j_{n,i},\ CSM \le CSM^j_{n,i}\right)\right], \qquad j = 1,\ 2,\ 3,\ \ldots,\ n-1 \tag{11}$$

From this formula, an $(n-1)$-member ensemble of the predicted SPI, SSMI and MSDI for the target month i could be derived. Then, based on this predicted ensemble, the occurrence probability (pp) of the drought could be estimated for any given threshold, as follows:

$$pp = \frac{n_x}{n} \tag{12}$$

where n_x represents the number of members below the given threshold x and n is the size of the predicted ensemble.

3.3. Prediction Evaluation

The Continuous Ranked Probability Score (CRPS) is a widely used tool for the probabilistic forecast verification [47]. The *CRPS* might be considered as the mean absolute error of the predicted ensemble, with a lower *CRPS* value indicating a higher forecasting accuracy. Here, the *CRPS* is used to

evaluate the predictive skill for different drought indicators with varying lead times. The *CRPS* might be expressed as:

$$CRPS = \int_{-\infty}^{+\infty} [F(x) - H(x - x_{OBS})]^2 dx \quad (13)$$

where $F(x)$ demonstrates the cumulative distribution function of the predicted drought index; x_{OBS} refers to the observed value; the integral variable x represents the drought index; finally, $H(x - x_{OBS})$ is the indicator function defined as:

$$H(x - x_{OBS}) = \begin{cases} 0\ (x < x_{OBS}) \\ 1\ (x \geq x_{OBS}) \end{cases} \quad (14)$$

4. Results

4.1. Data Validation

The accuracy of the MERRA-Land soil moisture data was examined based on the observed data from the agriculture stations (Shache and Wulawusu). As the units of the in situ and MERRA-Land data are different, we performed a validation by comparing their variations instead of the magnitudes. Figure 2 suggests that these two datasets showed similar fluctuations on a monthly scale. The correlation coefficients between the MERRA-Land and in situ data at the Shache and Wulawusu stations were approximately 0.54 and 0.49, respectively, which indicates that the MERRA-Land soil moisture product demonstrated a reasonable accuracy [37,48].

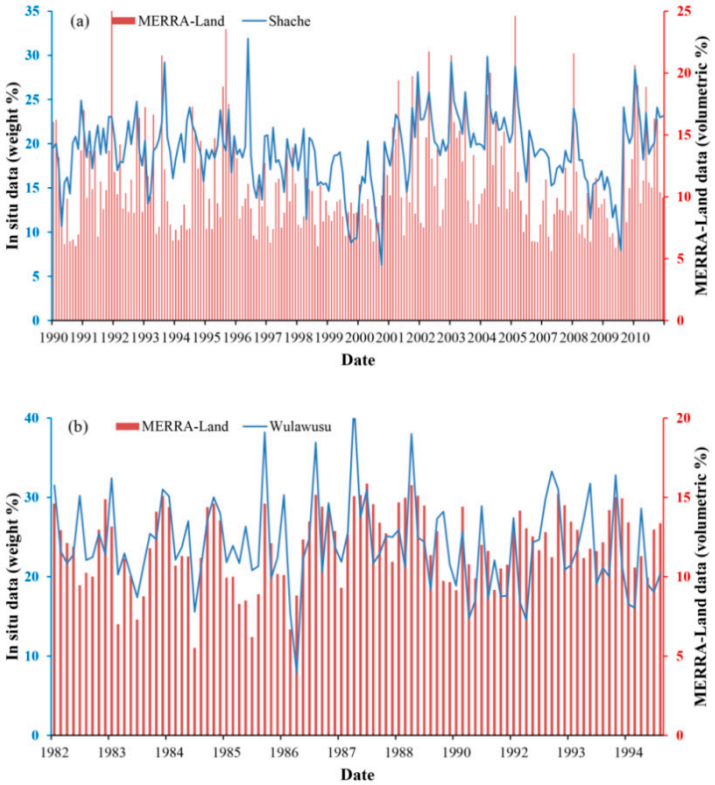

Figure 2. Monthly variations of the Modern-Era Retrospective analysis for Research and Applications (MERRA)-Land and in situ soil moisture data at the Shache (**a**) and Wulawusu (**b**) station.

The observed precipitation data from four weather stations (i.e., Aletai, Shache, Tieganlike and Tulufan) were utilized to evaluate the MERRA-Land product. Figure 3 depicts the agreement between these two datasets, with r^2 values of 0.75, 0.77, 0.83 and 0.73, respectively. The root mean square error (RMSE) values for the MERRA-Land precipitation amounted to 7.07 mm, 4.85 mm, 2.83 mm

and 1.82 mm, respectively. The MERRA-Land precipitation showed good agreement with the in situ observations.

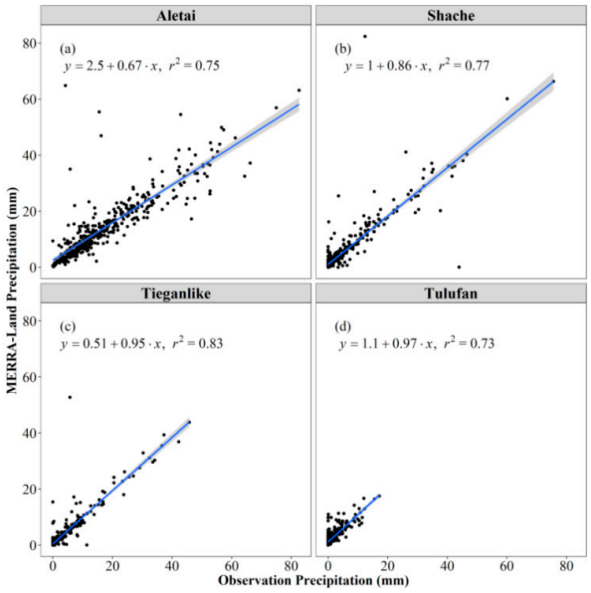

Figure 3. Scatterplots of the MERRA-Land precipitation data against the in situ data at the Aletai (**a**), Shache (**b**), Tieganlike (**c**) and Tulufan (**d**) station.

4.2. Spatial Patterns of Precipitation and Soil Moisture

In Figure 4a, the mean annual precipitation showed an uneven distribution pattern in Xinjiang. The minimum precipitation appeared in the centre of the Tarim basin, where the annual precipitation was less than 50 mm. The maximum precipitation is observed in the mountains of North Xinjiang, especially the Tianshan mountains where the annual precipitation exceeded 300 mm. Taking the Tianshan mountains as a middle boundary, the precipitation in South Xinjiang was lower than in North Xinjiang. Figure 4b represents the spatial pattern of the soil moisture, which ranged from 0.02 to 0.33 $m^3 \times m^{-3}$. The spatial pattern of the soil moisture was similar to that of the precipitation. A low soil moisture value was noticed in the centre of the Tarim and Junggar basins, while high values of soil moisture appeared in the mountainous areas between these two basins.

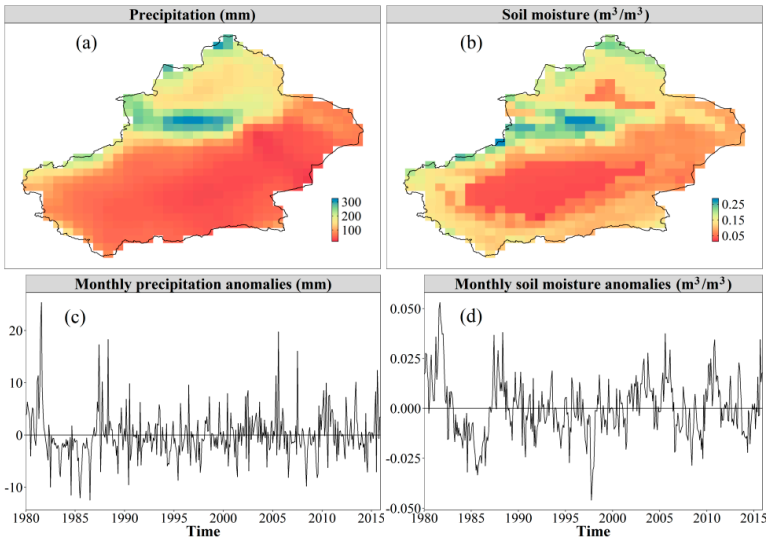

Figure 4. Spatial patterns and monthly anomalies of the precipitation (**a**,**c**) and soil moisture (**b**,**d**).

The monthly precipitation and soil moisture deviations from the monthly historical average during the period 1980–2015 were shown in Figure 4c,d. Regarding the precipitation, the monthly value measured less than the historical average in about 56% of the calculated months and these months were mainly situated in the periods 1982–1986, 1988–1992, 1994–1997, 1999–2001, 2007–2009 and 2012–2014. For the soil moisture, the monthly value was less than the historical average in about 53% of the months and these appeared mainly in the periods 1983–1986, 1989–1992, 1994–2001, 2006–2009 and 2012–2014. A low monthly precipitation or soil moisture value, which was deviated from the monthly historical average to a certain extent, might lead to a drought.

4.3. Drought Monitoring

4.3.1. Time Series of Various Drought Indicators

Figure 5 demonstrates the historical time series of the spatially averaged SPI, SSMI and MSDI for the period 1980–2015. During this period, 132, 132 and 171 months appeared to be under drought for the SPI, SSMI and MSDI, respectively. Concerning those, 27%, 27% and 33% suffered from severe drought (D2) for these three indicators, respectively. In the study area, the drought occurred every 2.3 years on average. These three indicators were generally consistent and could monitor these severe drought events, which occurred during 1983–1986, 1997–1998, 2008, 2009 and 2014. These drought events have been reported. For example, severe drought took place in 1983, affecting 3.8×10^5 hm^2 of the farmlands and 6.67×10^6 hm^2 of the grasslands [49]. In 2008, about 1.86×10^7 hm^2 grasslands experienced drought and it even restricted the area's domestic water supply [50]. As reported by the Uygur Autonomous Regional Meteorological Service, Xinjiang also suffered from a severe drought disaster in 2014, which caused a direct economic loss of nearly RMB 2.89 billion, ranking the first in the same historical period. Other drought events were also confirmed in various drought statistical yearbooks from China and the Xinjiang Uygur Autonomous Region.

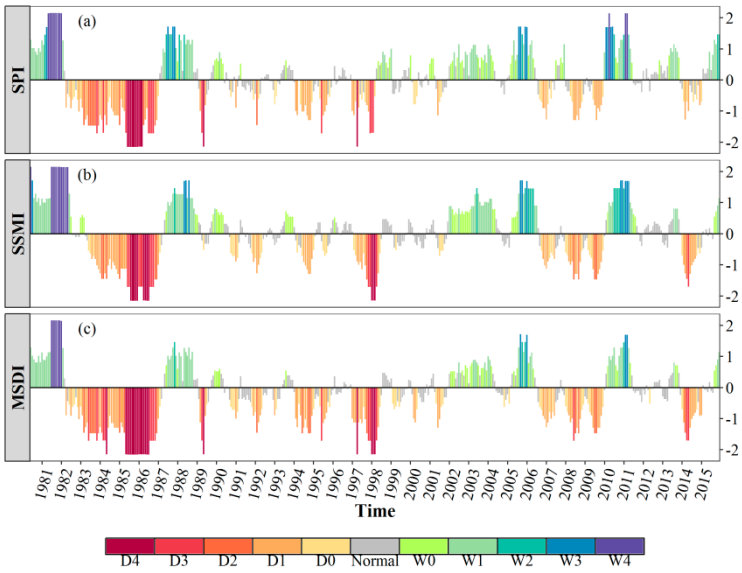

Figure 5. Time series of the spatially averaged Standardized Precipitation Index (SPI) (**a**), Soil Moisture Index (SSMI) (**b**) and Multivariate Standardized Drought Index (MSDI) (**c**).

However, there are still discrepancies among these three indicators regarding the drought onset, persistence and severity. For example, for the drought events which occurred in 1983–1986 and 1997–1998, the SPI and MSDI monitored the drought a few months earlier than the SSMI, which might be due to the fact that the soil moisture deficit originated from the precipitation deficit. During the monitoring period, the mean drought persistence amounted to 8.25 and 9.42 months for the SPI and SSMI, respectively. This finding is consistent with previous studies, which found that the soil moisture

is superior to the precipitation when it is used to monitor the drought persistence [15,51]. The MSDI, calculated from the joint probability distribution, could incorporate the characteristics of both the soil moisture and precipitation. It is suspected that the drought severity captured by the MSDI would be more severe than either the SPI or SSMI, when both these indices indicated a drought [52]. In this study, the mean drought peak for the MSDI measured −1.21, which was heavier than either the SPI (−1.13) or SSMI (−1.14).

In addition, the SPI and SSMI indicated different signals across several time steps. For example, in 1982 and 1989, the SPI indicated moderate to exceptional droughts, while the SSMI proved normal or even wet conditions. Such discrepancies might be due to the relatively wet soil conditions in the early stage and the below-average precipitation throughout a period that caused the soil to stay wet [9].

4.3.2. Spatial Pattern of Droughts during the Period April–July 2014

April to July is an important agricultural period in Xinjiang. Therefore, as an example of monitoring spatial drought information based on the SPI, SSMI and MSDI, we examined a drought that happened from April to July 2014. Since there are no observed drought data available in China, we could only compare the differences among these three indicators, rather than evaluate their accuracy. As shown in Figure 6, the drought during this period was generally depicted by these three indicators, but the spatial coverage, as well as the drought persistence, varied according to different indicators.

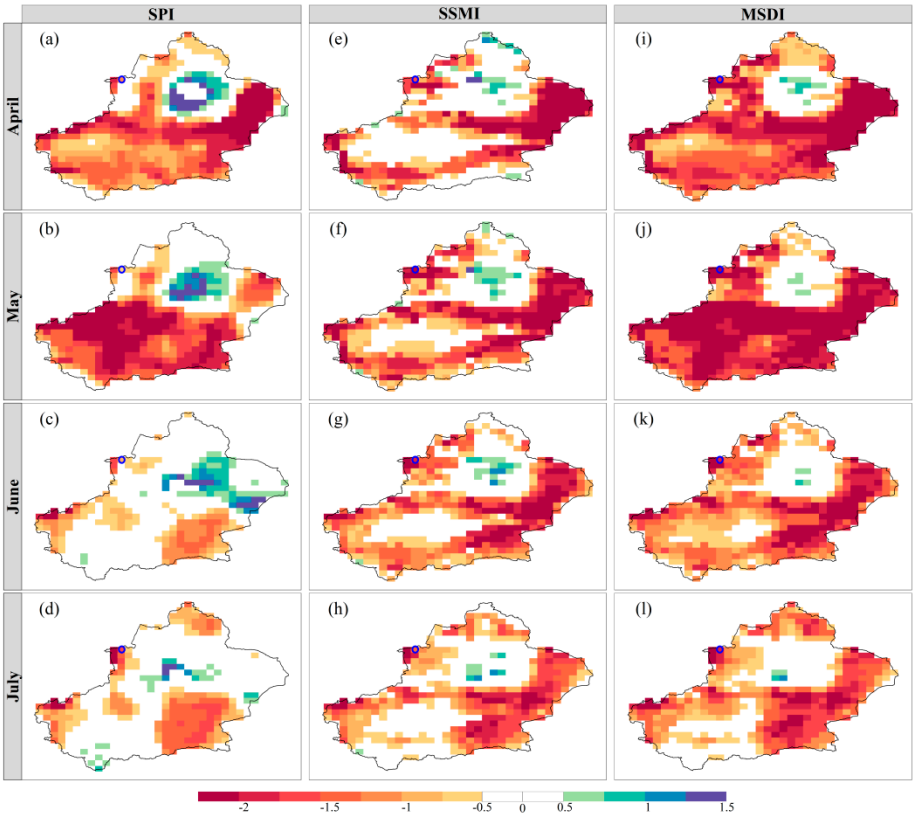

Figure 6. Drought monitoring based on the SPI (**a**–**d**), SSMI (**e**–**h**) and MSDI (**i**–**l**) for April–July 2014.

In Figure 6a, the SPI indicated a D4 drought (SPI < −2) in the east of North Xinjiang, whereas most areas in South Xinjiang were located in the D0 to D1 drought category (−0.5 < SPI < −1.3) in April. In May (Figure 6b), the drought conditions relieved in North Xinjiang, while aggravated in South Xinjiang. Only the eastern regions and western marginal areas of South Xinjiang, however, showed a D0 to D1 drought in June and July (Figure 6c,d).

The agricultural drought (SSMI) area does not entirely match the meteorological drought (SPI) areas. As shown in Figure 6e–h, the agricultural drought based on the SSMI was mainly distributed

in the boundary regions of South Xinjiang, and the eastern and western regions of North Xinjiang. Regarding the eastern regions of North Xinjiang, the SSMI demonstrated a D4 drought in April, which was consistent with the SPI. The drought conditions in these regions gradually relieved but did not disappear. By July, the SSMI still captured a D0 to D1 drought in the east of North Xinjiang. Meanwhile, based on the SSMI, the drought in South Xinjiang had aggravated from April to May and then gradually relieved but at a slower drought mitigation rate than the one based on the SPI. In other words, the SSMI indicated a longer drought persistence than the SPI.

Moreover, the MSDI described droughts in areas where either the SPI or SSMI illustrated a deficit, thus it exhibited a larger area under drought conditions compared to the SPI and SSMI (Figure 6i–l). In order to compare the drought severity among these three indicators, a grid cell (81° E, 45° N) in the western part of North Xinjiang was considered as an example. The location is marked with a blue circle in Figure 6. The MSDI values in this grid measure −1.7, −2.1, −1.7 and −1.7 for April, May, June and July, respectively. The SPI values amount to −1.0, −0.6, −0.8 and −1.4, and the SSMI values are −1.4, −2.1, −1.7 and −1.2. The results are in step with previous studies, which indicated that the Multivariate Standardized Drought Index (MSDI) has been showing more severe drought conditions than the univariate drought indices (i.e., the SPI and SSMI) [52,53]. Furthermore, the MSDI exhibited a similar drought persistence as the SSMI, which was longer than the SPI.

4.4. Drought Prediction

In a drought early warning system, the drought conditions situated below the moderate level (D1, index < −0.8) are of a critical concern. As shown in Figure 6, the drought during May 2014 was more severe than that in the other months. We took the drought in May 2014 as an example so as to predict the droughts and to provide the probability of drought occurrence below the D1 level at different lead times based on the SPI, SSMI and MSDI, respectively. For a contrastive analysis, the monitored drought conditions below the D1 level based on the SPI, SSMI and MSDI for May 2014 have been sketched in Figure 7.

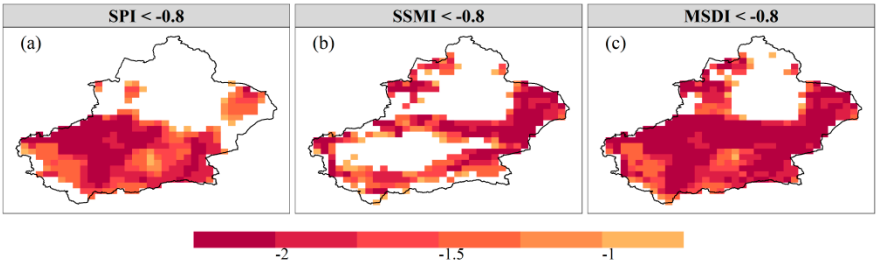

Figure 7. Monitored drought conditions below D1 based on the SPI (**a**), SSMI (**b**) and MSDI (**c**) for May 2014.

The drought probability forecasts at different lead times based on the SPI are presented in Figure 8a–d. The 1-month lead predictive map resembles the monitored map (Figure 7a) in terms of the spatial extent. The areas with a relatively high probability (~70%) were mainly distributed in the east of North Xinjiang and the northwest of South Xinjiang. The probability for most parts of South Xinjiang was calculated around 50%. However, the predictive skill dropped off gradually after a 1-month lead time. For the 2-month, 3-month and 4-month lead times, the probability rate for almost all regions was less than 50% or even lower. In other words, there was a moderate predictive skill that was visible up to a 1-month lead time, but almost no significant predictive skill after a 1-month lead time. The Continuous Ranked Probability Score (CRPS) delivers an integrated evaluation of the accuracy and reliability of the predicted ensemble. A lower CRPS value indicates a higher forecasting accuracy and vice versa. Figure 8e–h illustrates the spatial patterns of the CRPS at different lead times. As shown, the spatially averaged CRPS values amounted to 0.376, 0.558, 0.656 and 0.680 at lead times of 1-, 2-, 3- and 4-month, respectively, which signifies that the mean absolute errors increased with the

lead time. From the spatial distribution, the regions suffering from more severe drought conditions (e.g., the northwest patches of South Xinjiang) illustrated higher CRPS values than the other areas. Figure 8i–l represents the predicted ensemble median against the monitored SPI for each grid in the study area at different lead times. The r^2 value was 0.6 at a 1-month lead time and decreased sharply after a 1-month lead time. There was little correlation between the monitored SPI and the predicted ensemble median at 3- and 4-month lead times. At different lead times, the predicted ensemble median generally underestimated the drought/wet conditions and the degree of underestimation intensified with the increase in lead time.

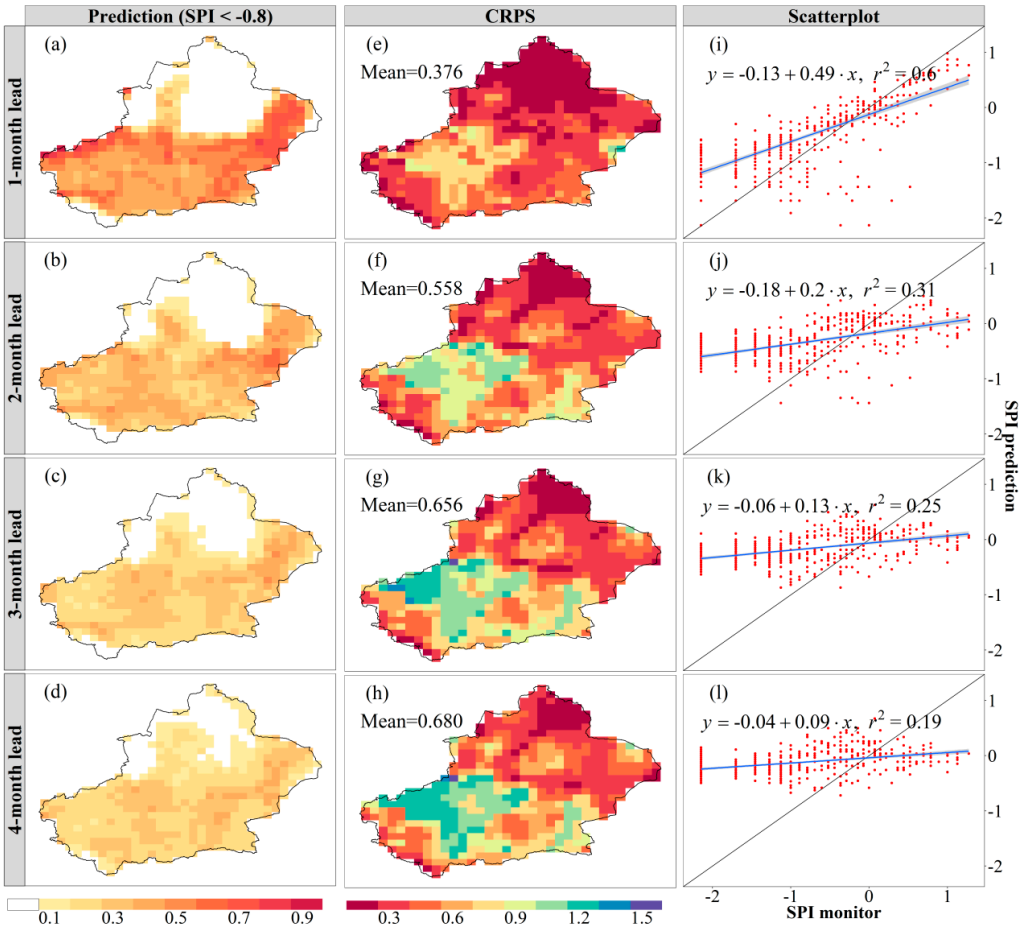

Figure 8. Drought probability predictions and probabilistic prediction evaluations based on the SPI at a 1-month lead (**a**,**e**,**i**), 2-month lead (**b**,**f**,**j**), 3-month lead (**c**,**g**,**k**) and 4-month lead (**d**,**h**,**l**) for May 2014.

Figure 9a–d provides the 1- to 4-month lead forecasts based on the SSMI. The visual comparisons between the drought predictions and monitored droughts for the 1- and 2-month leads (Figure 7b) reveal that regions with a high probability (~90%) are consistent with the monitored drought conditions. The SSMI 3-month lead prediction described a high drought probability (~80%) in the east of North Xinjiang and some parts of South Xinjiang, while the 4-month lead prediction showed limited skills across most regions. As expected, the spatially averaged CRPS values augmented with the lead time (Figure 9e–h). For the 1- and 2-month forecasts, the CRPS values in most areas measured lower than 0.5. Overall, the CRPS values across the marginal areas of South Xinjiang were higher than in other areas. Furthermore, Figure 9i–l denotes a relatively good agreement between the predicted ensemble median and the monitored SSMI, with r^2 of 0.89, 0.75, 0.65 and 0.58 for various lead times. As noticed in Figure 9i at a 1-month lead time, the predicted ensemble median and the monitored drought are generally laid along the 1:1 line, which presents a high degree of consistency. However, the ensemble

median of the 1-month lead prediction underestimated the droughts while overestimating the wet conditions. As the lead time rose, the degree of drought underestimation gradually intensified.

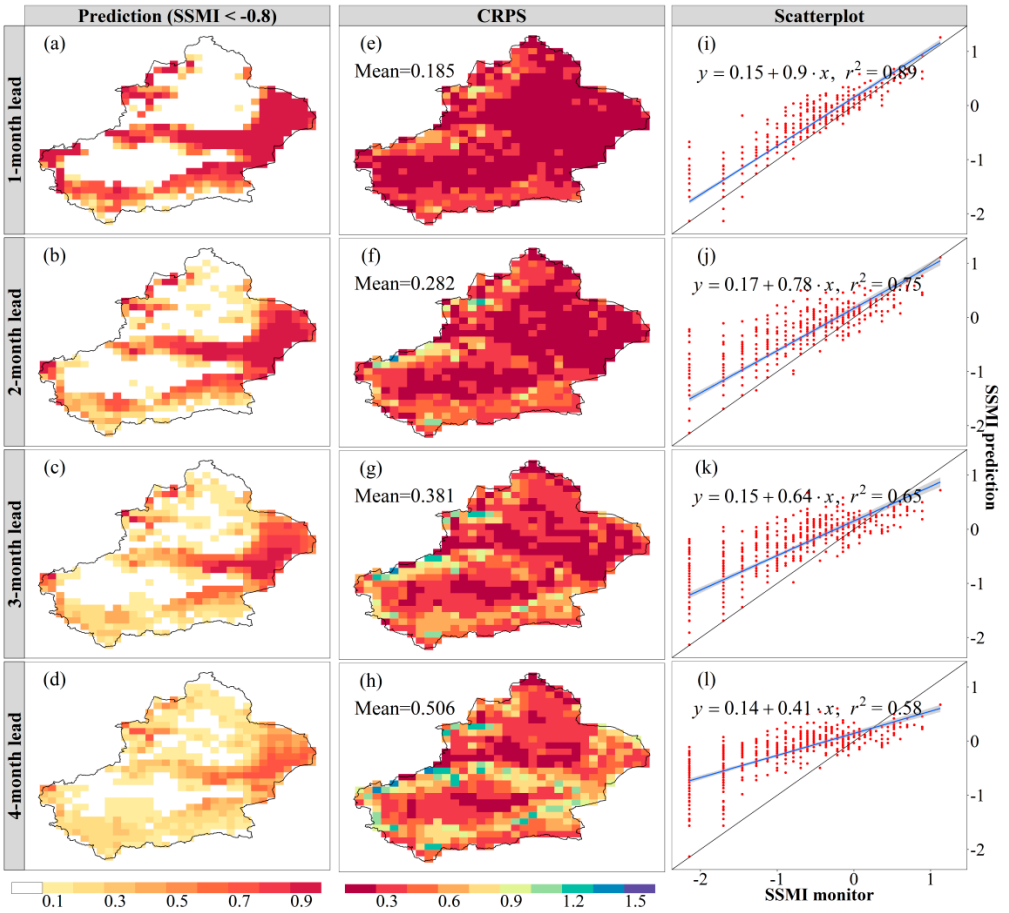

Figure 9. Drought probability predictions and probabilistic prediction evaluations based on the SSMI at a 1-month lead (**a**,**e**,**i**), 2-month lead (**b**,**f**,**j**), 3-month lead (**c**,**g**,**k**) and 4-month lead (**d**,**h**,**l**) for May 2014.

The predicted drought probability results based on the MSDI for the 1- to 4-month lead times are presented in Figure 10a–d. The results suggest that the areas where droughts were predicted with a high probability at a 1-month lead time were consistent with the monitored droughts shown in Figure 7c. Additionally, the predictive skill was higher in the east of Xinjiang, with a drought probability exceeding 90%. The 2-month lead forecast could only monitor the drought conditions in the middle and eastern parts of Xinjiang and there was little skill at lead times of 3–4 months. The spatially averaged CRPS values in longer leads (i.e., 3- and 4-month) were larger than those in shorter leads (i.e., 1- and 2-month). Most parts of South Xinjiang exhibited lower predictive skills and a higher uncertainty with relatively high CRPS values. At the 1-month lead time, a good agreement was noticed between the predicted ensemble median and the monitored MSDI, with r^2 measuring 0.73. The relation between the predicted ensemble median and the monitored MSDI became more scattered with the increases in lead time. Similar to the SPI and SSMI, the predicted ensemble median based on the MSDI underestimated the drought degree.

The comparisons of Figures 8–10 reveal a longer lead time predictability for the SSMI and MSDI relative to the SPI. With regard to the CRPS (i.e., the mean absolute errors), the value was higher than 0.5 at the 2-month lead time for the SPI, while it was higher than 0.5 at a lead time of 4- and 3-month regarding the SSMI and MDSI, respectively. For the r^2 value, the predicted ensemble median against the monitored drought severity was lower than 0.5 at the 2-month lead time for the SPI and MSDI, while it was still higher than 0.5 at a lead time of 4-month for the SSMI. In summary, the SPI provided relatively

reasonable predictions at a 1-month lead time while the predictive skill maintained up to 2-month and 3-month lead times for the MSDI and SSMI, respectively. In addition, for these three indicators, the predicted ensemble median generally underestimated the monitored drought degree. Hence, it would be better to predict in a probabilistic way, rather than using the deterministic forecasting.

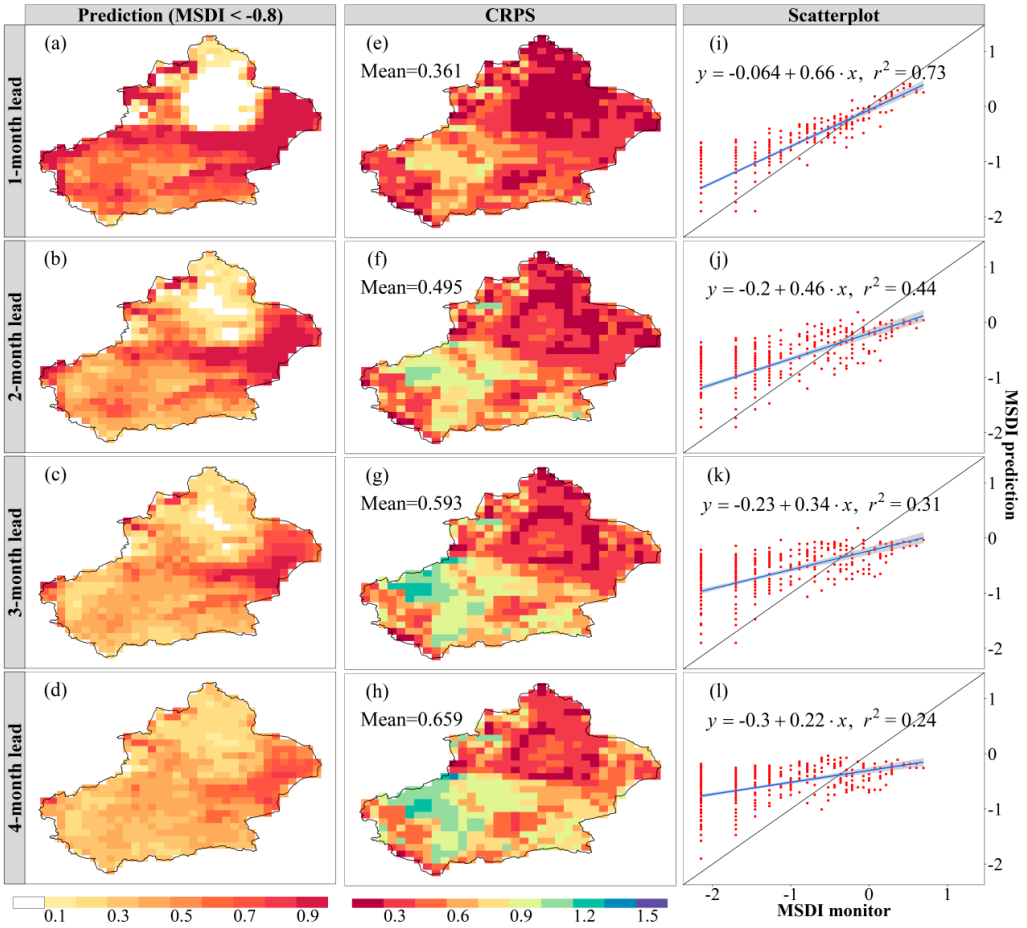

Figure 10. Drought probability predictions and probabilistic prediction evaluations based on the MSDI at a 1-month lead (**a**,**e**,**i**), 2-month lead (**b**,**f**,**j**), 3-month lead (**c**,**g**,**k**) and 4-month lead (**d**,**h**,**l**) for May 2014.

5. Discussion

As a monitoring tool, since the SPI characterizes the deficit in precipitation, the drought based on the SPI may develop quickly and end abruptly due to the high variability in precipitation [16,54]. The SSMI, on the other hand, represents the deficit in the soil moisture, which might arise from either a low precipitation or a high evapotranspiration [55]. As the soil moisture responds to the precipitation with some time lags [14], the drought based on the SSMI does not totally match the one based on the SPI. Furthermore, compared to the individual drought index, the MSDI describes the joint distribution of the soil moisture and precipitation and might therefore be used to characterize the overall drought conditions [9,53].

As a prediction tool, the SSMI performs better for the long-term drought predictions than the SPI. This was illustrated by examining the persistence of the cumulative soil moisture against that of cumulative precipitation in Figure 11, which shows the autocorrelations of the 6-month cumulative soil moisture and precipitation at 1- to 5-month time lags. Generally, the autocorrelation of the cumulative soil moisture was higher than that of the cumulative precipitation. With the increase in lag times, the autocorrelation of the cumulative soil moisture decayed more slowly compared to the cumulative

precipitation. The median of the autocorrelation coefficients for the cumulative soil moisture exceeded 0.5, even at a 3-month lag, while for cumulative precipitation it fell below 0.5 after a 2-month lag. Previous studies also illustrated that the precipitation has a high variability, while the soil moisture persistence could span weeks to a couple of months, and the cumulative soil moisture has a longer persistence based on the temporal integration of data [56–58]. The long persistence of the cumulative soil moisture is important to improve the drought predictive skills and might lead to a better prediction based on the SSMI than the SPI.

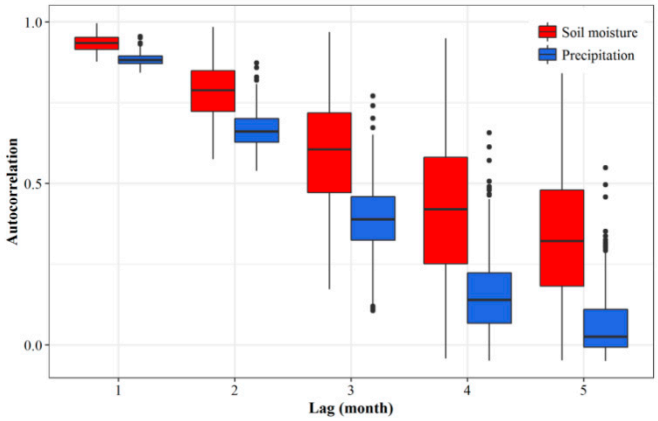

Figure 11. Box plot of the autocorrelation coefficients for the 6-month cumulative soil moisture (**red**) and precipitation (**blue**) at different time lags.

Furthermore, for the prediction based on the same drought index at the same lead time, the CRPS value demonstrated a spatial heterogeneity (Figures 8–10), which means that the prediction ability varied spatially. The difference in the prediction ability might arise from the difference in drought levels between the spatial units. In order to confirm this, we calculated the CRPS value corresponding to the different drought indicators while predicting the different levels of drought. As shown in Figure 12, with the aggravation in drought severity, the SPI-based and MSDI-based drought prediction ability weakened, as reflected by the rising CRPS value. The decay rate of the prediction ability based on the MSDI was lower than the one based on the SPI. The drought prediction based on the SSMI illustrated a relatively stable prediction ability for different drought levels. The difference in prediction ability could be related to a high variability in precipitation and a long persistence of soil moisture. Especially, the soil moisture in dry conditions has a longer persistence than that in wet conditions [59] and the precipitation in dry areas has a bigger variability compared to that in wet areas [60]. Based on the above analysis, the spatial variation of the CRPS in Figures 8 and 10 could be explained. The drought situation in South Xinjiang was more severe than that in North Xinjiang during May 2014 (Figure 6), which caused a higher CRPS value in South Xinjiang than in North Xinjiang.

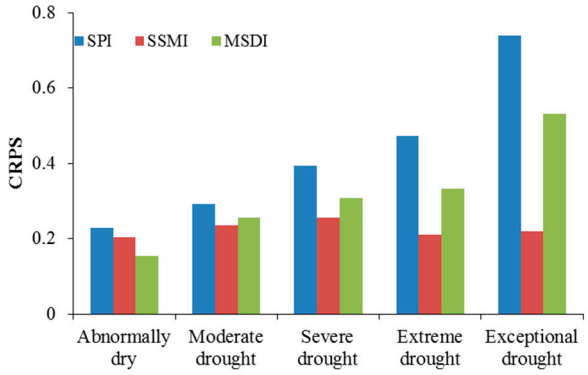

Figure 12. Evaluation of the different drought indices for predicting different drought levels.

6. Conclusions

Based on the soil moisture and precipitation data from the MERRA-Land dataset, multiple indicators were calculated to monitor and predict droughts in Xinjiang, China. Generally, the spatially averaged SPI, SSMI and MSDI could capture severe historical drought events and indicated that the droughts happened every 2.3 years on average. However, the spatial coverage, persistence and severity of the drought varied with different indicators. The drought monitoring for the period April–July 2014 demonstrated that the meteorological drought based on the SPI was mainly distributed in South Xinjiang and only persisted for a short time. The agricultural drought based on the SSMI was located in the boundary regions of South Xinjiang and the east of North Xinjiang, and also had a longer persistence. The MSDI characterized the overall drought conditions based on the state of both the soil moisture and precipitation.

Additionally, the ESP method was used to predict the probability of the drought occurrence (below D1 level) at different lead times based on the SSMI, SPI and MSDI, respectively. The results illustrate that the 1-month lead forecast for these three indicators was the most accurate, and the predictive skill gradually decayed as the lead time increased. For the SPI, there were large uncertainties visible in the predictions and almost no predictive skills beyond a 1-month lead. For the MSDI, the reasonable predictive skill was found at lead times of 1–2 months. For the SSMI, the predictive skill could be maintained up to a 3-month lead due to the long persistence of the soil moisture.

In short, we could see that the choice of the drought index depends on the specific problem. The MSDI proves better for the drought monitoring than the univariate drought indices (i.e., the SPI, SSMI), while the SSMI has more advantages regarding the drought prediction.

Author Contributions: Conceptualization, Y.W. and J.Y.; Methodology, Y.W.; Software, J.Y.; Validation, Y.C.; Formal analysis, Z.S.; Writing—original draft preparation, Y.W.; Visualization, P.D.M.; Supervision, J.Y. Writing—Review and Editing, B.L. and H.G. All authors have read and agreed to the published version of the manuscript.

Funding: This research was funded by the National Key Research and Development Program (2019YFA0606902), the Key Research Program of the Chinese Academy of Sciences (ZDRW-ZS-2019-3) and the Chinese Academy of Sciences President's International Fellowship Initiative (PIFI) (Grant No. 2017VCA0002).

Acknowledgments: The authors thank S. Cnudde for the language editing.

Conflicts of Interest: The authors declare no conflict of interest.

References

1. Dutra, E.; Pozzi, W.; Wetterhall, F.; Giuseppe, F.D.; Magnusson, L.; Naumann, G.; Barbosa, P.; Vogt, J.; Pappenberger, F. Global meteorological drought–Part 2: Seasonal forecasts. *Hydrol. Earth Syst. Sci.* **2014**, *18*, 2669–2678. [CrossRef]
2. Conforti, P.; Ahmed, S.; Markova, G. *Impact of Disasters and Crises on Agriculture and Food Security, 2017*; FAO: Rome, Italy, 2018.
3. Dai, A. Drought under global warming: A review. *Wiley Interdiscip. Rev. Clim. Chang.* **2011**, *2*, 45–65. [CrossRef]
4. Dai, A. Increasing drought under global warming in observations and models. *Nat. Clim. Chang.* **2013**, *3*, 52–58. [CrossRef]
5. Mishra, A.K.; Singh, V.P. A review of drought concepts. *J. Hydrol.* **2010**, *391*, 202–216. [CrossRef]
6. Lyon, B.; Bell, M.A.; Tippett, M.K.; Kumar, A.; Hoerling, M.P.; Quan, X.-W.; Wang, H. Baseline probabilities for the seasonal prediction of meteorological drought. *J. Appl. Meteorol. Climatol.* **2012**, *51*, 1222–1237. [CrossRef]
7. Trenberth, K.E.; Dai, A.; Van Der Schrier, G.; Jones, P.D.; Barichivich, J.; Briffa, K.R.; Sheffield, J. Global warming and changes in drought. *Nat. Clim. Chang.* **2014**, *4*, 17–22. [CrossRef]
8. McKee, T.B.; Doesken, N.J.; Kleist, J. The relationship of drought frequency and duration to time scales. In Proceedings of the 8th Conference on Applied Climatology, Anaheim, CA, USA, 17–22 January 1993; pp. 179–183.

9. Hao, Z.; AghaKouchak, A. Multivariate standardized drought index: A parametric multi-index model. *Adv. Water Resour.* **2013**, *57*, 12–18. [CrossRef]
10. Shukla, S.; Wood, A.W. Use of a standardized runoff index for characterizing hydrologic drought. *Geophys. Res. Lett.* **2008**, *35*. [CrossRef]
11. Vicente-Serrano, S.M.; Beguería, S.; López-Moreno, J.I. A multiscalar drought index sensitive to global warming: The standardized precipitation evapotranspiration index. *J. Clim.* **2010**, *23*, 1696–1718. [CrossRef]
12. Xia, Y.; Ek, M.B.; Peters-Lidard, C.D.; Mocko, D.; Svoboda, M.; Sheffield, J.; Wood, E.F. Application of USDM statistics in NLDAS-2: Optimal blended NLDAS drought index over the continental United States. *J. Geophys. Res. Atmos.* **2014**, *119*, 2947–2965. [CrossRef]
13. Hao, Z.; AghaKouchak, A.; Nakhjiri, N.; Farahmand, A. Global integrated drought monitoring and prediction system. *Sci. Data* **2014**, *1*, 140001. [CrossRef]
14. Mo, K.C. Drought onset and recovery over the United States. *J. Geophys. Res. Atmos.* **2011**, *116*. [CrossRef]
15. Cook, E.R.; Seager, R.; Cane, M.A.; Stahle, D.W. North American drought: Reconstructions, causes, and consequences. *Earth-Sci. Rev.* **2007**, *81*, 93–134. [CrossRef]
16. Heim, R.R., Jr. A review of twentieth-century drought indices used in the United States. *Bull. Am. Meteorol. Soc.* **2002**, *83*, 1149–1165. [CrossRef]
17. Mishra, A.K.; Singh, V.P. Drought modeling—A review. *J. Hydrol.* **2011**, *403*, 157–175. [CrossRef]
18. Hao, Z.; Yuan, X.; Xia, Y.; Hao, F.; Singh, V.P. An overview of drought monitoring and prediction systems at regional and global scales. *Bull. Am. Meteorol. Soc.* **2017**, *98*, 1879–1896. [CrossRef]
19. Özger, M.; Mishra, A.K.; Singh, V.P. Long lead time drought forecasting using a wavelet and fuzzy logic combination model: A case study in Texas. *J. Hydrometeorol.* **2012**, *13*, 284–297. [CrossRef]
20. Hao, Z.; Hao, F.; Xia, Y.; Singh, V.P.; Hong, Y.; Shen, X.; Ouyang, W. A statistical method for categorical drought prediction based on NLDAS-2. *J. Appl. Meteorol. Climatol.* **2016**, *55*, 1049–1061. [CrossRef]
21. Yuan, X.; Wood, E.F. Multimodel seasonal forecasting of global drought onset. *Geophys. Res. Lett.* **2013**, *40*, 4900–4905. [CrossRef]
22. Nijssen, B.; Shukla, S.; Lin, C.; Gao, H.; Zhou, T.; Sheffield, J.; Wood, E.F.; Lettenmaier, D.P. A prototype global drought information system based on multiple land surface models. *J. Hydrometeorol.* **2014**, *15*, 1661–1676. [CrossRef]
23. Kirtman, B.; Anderson, D.; Brunet, G.; Kang, I.-S.; Scaife, A.A.; Smith, D. Prediction from weeks to decades. In *Climate science for Serving Society*; Springer: Dordrecht, The Netherlands, 2013; pp. 205–235.
24. Smith, D.M.; Scaife, A.A.; Kirtman, B.P. What is the current state of scientific knowledge with regard to seasonal and decadal forecasting? *Environ. Res. Lett.* **2012**, *7*, 015602. [CrossRef]
25. Schepen, A.; Wang, Q.; Robertson, D.E. Combining the strengths of statistical and dynamical modeling approaches for forecasting Australian seasonal rainfall. *J. Geophys. Res. Atmos.* **2012**, *117*. [CrossRef]
26. Stockdale, T.N.; Alves, O.; Boer, G.; Deque, M.; Ding, Y.; Kumar, A.; Kumar, K.; Landman, W.; Mason, S.; Nobre, P. Understanding and predicting seasonal-to-interannual climate variability-the producer perspective. *Procedia Environ. Sci.* **2010**, *1*, 55–80. [CrossRef]
27. Schepen, A.; Wang, Q. Model averaging methods to merge operational statistical and dynamic seasonal streamflow forecasts in Australia. *Water Resour. Res.* **2015**, *51*, 1797–1812. [CrossRef]
28. Cao, Y.; Nan, Z.; Cheng, G. GRACE gravity satellite observations of terrestrial water storage changes for drought characterization in the arid land of northwestern China. *Remote Sens.* **2015**, *7*, 1021–1047. [CrossRef]
29. Wang, H.; Chen, Y.; Chen, Z. Spatial distribution and temporal trends of mean precipitation and extremes in the arid region, northwest of China, during 1960–2010. *Hydrol. Process.* **2013**, *27*, 1807–1818. [CrossRef]
30. Zhang, Q.; Sun, P.; Li, J.; Xiao, M.; Singh, V.P. Assessment of drought vulnerability of the Tarim River basin, Xinjiang, China. *Theor. Appl. Climatol.* **2015**, *121*, 337–347. [CrossRef]
31. Zhang, Q.; Sun, P.; Li, J.; Singh, V.P.; Liu, J. Spatiotemporal properties of droughts and related impacts on agriculture in Xinjiang, China. *Int. J. Climatol.* **2015**, *35*, 1254–1266. [CrossRef]
32. Zhang, Q.; Li, J.; Singh, V.P.; Bai, Y. SPI-based evaluation of drought events in Xinjiang, China. *Nat. Hazards* **2012**, *64*, 481–492. [CrossRef]
33. AghaKouchak, A. A baseline probabilistic drought forecasting framework using standardized soil moisture index: Application to the 2012 United States drought. *Hydrol. Earth Syst. Sci.* **2014**, *18*, 2485–2492. [CrossRef]

34. Trambauer, P.; Maskey, S.; Winsemius, H.; Werner, M.; Uhlenbrook, S. A review of continental scale hydrological models and their suitability for drought forecasting in (sub-Saharan) Africa. *Phys. Chem. Earth Parts A/B/C* **2013**, *66*, 16–26. [CrossRef]
35. Yoon, J.-H.; Mo, K.; Wood, E.F. Dynamic-model-based seasonal prediction of meteorological drought over the contiguous United States. *J. Hydrometeorol.* **2012**, *13*, 463–482. [CrossRef]
36. Lavers, D.; Luo, L.; Wood, E.F. A multiple model assessment of seasonal climate forecast skill for applications. *Geophys. Res. Lett.* **2009**, *36*. [CrossRef]
37. Wang, Y.; Yang, J.; Chen, Y.; Wang, A.; De Maeyer, P. The spatiotemporal response of soil moisture to precipitation and temperature changes in an Arid Region, China. *Remote Sens.* **2018**, *10*, 468. [CrossRef]
38. Liang, S.; Yi, Q.; Liu, J. Vegetation dynamics and responses to recent climate change in Xinjiang using leaf area index as an indicator. *Ecol. Indic.* **2015**, *58*, 64–76.
39. Kottek, M.; Grieser, J.; Beck, C.; Rudolf, B.; Rubel, F. World map of the Köppen-Geiger climate classification updated. *Meteorol. Z.* **2006**, *15*, 259–263. [CrossRef]
40. Liu, Y.-L.; Luo, K.-L.; Lin, X.-X.; Gao, X.; Ni, R.-X.; Wang, S.-B.; Tian, X.-L. Regional distribution of longevity population and chemical characteristics of natural water in Xinjiang, China. *Sci. Total Environ.* **2014**, *473*, 54–62. [CrossRef]
41. Luo, M.; Liu, T.; Frankl, A.; Duan, Y.; Meng, F.; Bao, A.; Kurban, A.; De Maeyer, P. Defining spatiotemporal characteristics of climate change trends from downscaled GCMs ensembles: How climate change reacts in Xinjiang, China. *Int. J. Climatol.* **2018**, *38*, 2538–2553. [CrossRef]
42. Global Modeling and Assimilation Office. *Tavgm_2d_mld_Nx: MERRA Simulated 2D Incremental Analysis Update (IAU) MERRA-Land Reanalysis, GEOSldas-MERRALand, Time Average Monthly Mean V5.2.0*; Goddard Earth Sciences Data and Information Services Center (GES DISC): Greenbelt, MD, USA, 2008.
43. Gringorten, I.I. A plotting rule for extreme probability paper. *J. Geophys. Res.* **1963**, *68*, 813–814. [CrossRef]
44. Svoboda, M.; LeComte, D.; Hayes, M.; Heim, R.; Gleason, K.; Angel, J.; Rippey, B.; Tinker, R.; Palecki, M.; Stooksbury, D.; et al. The drought monitor. *Bull. Am. Meteor. Soc.* **2002**, *83*, 1181–1190. [CrossRef]
45. Wood, A.W.; Lettenmaier, D.P. An ensemble approach for attribution of hydrologic prediction uncertainty. *Geophys. Res. Lett.* **2008**, *35*. [CrossRef]
46. Day, G.N. Extended streamflow forecasting using NWSRFS. *J. Water Resour. Plan. Manag.* **1985**, *111*, 157–170. [CrossRef]
47. Bourdin, D.R.; Nipen, T.N.; Stull, R.B. Retracted: Reliable probabilistic forecasts from an ensemble reservoir inflow forecasting system. *Water Resour. Res.* **2014**, *50*, 3108–3130. [CrossRef]
48. Su, B.; Wang, A.; Wang, G.; Wang, Y.; Jiang, T. Spatiotemporal variations of soil moisture in the Tarim River basin, China. *Int. J. Appl. Earth Obs. Geoinf.* **2016**, *48*, 122–130. [CrossRef]
49. Bai, Y.; Musha, R.; Lei, X.; Zhang, J. Analysis on characteristic and affecting factor of drought disaster of Xinjiang. *Yellow River* **2012**, *34*, 61–63.
50. Ma, Y.; Taxifulati, T.; Liu, X.; Lu, G. application of multitemporal SPOT satellite imagery to monitoring extraodinarity serious drought in 2008. *Xinjiang Agric. Sci.* **2009**, *46*, 1098–1102.
51. Seager, R.; Kushnir, Y.; Herweijer, C.; Naik, N.; Velez, J. Modeling of tropical forcing of persistent droughts and pluvials over western North America: 1856–2000. *J. Clim.* **2005**, *18*, 4065–4088. [CrossRef]
52. Hao, Z.; Hao, F.; Singh, V.P.; Ouyang, W.; Cheng, H. An integrated package for drought monitoring, prediction and analysis to aid drought modeling and assessment. *Environ. Model. Softw.* **2017**, *91*, 199–209. [CrossRef]
53. Hao, Z.; AghaKouchak, A. A nonparametric multivariate multi-index drought monitoring framework. *J. Hydrometeorol.* **2014**, *15*, 89–101. [CrossRef]
54. Mo, K.C.; Shukla, S.; Lettenmaier, D.P.; Chen, L.C. Do Climate Forecast System (CFSv2) forecasts improve seasonal soil moisture prediction. *Geophys. Res. Lett.* **2012**, *39*. [CrossRef]
55. Luo, L.; Apps, D.; Arcand, S.; Xu, H.; Pan, M.; Hoerling, M. Contribution of temperature and precipitation anomalies to the California drought during 2012–2015. *Geophys. Res. Lett.* **2017**, *44*, 3184–3192. [CrossRef]
56. Koster, R.D.; Mahanama, S.; Yamada, T.; Balsamo, G.; Berg, A.; Boisserie, M.; Dirmeyer, P.; Doblas-Reyes, F.; Drewitt, G.; Gordon, C. Contribution of land surface initialization to subseasonal forecast skill: First results from a multi-Model experiment. *Geophys. Res. Lett.* **2010**, *37*. [CrossRef]
57. Nicolai-Shaw, N.; Gudmundsson, L.; Hirschi, M.; Seneviratne, S.I. Long-term predictability of soil moisture dynamics at the global scale: Persistence versus large-scale drivers. *Geophys. Res. Lett.* **2016**, *43*, 8554–8562. [CrossRef]

58. Dirmeyer, P.A.; Schlosser, C.A.; Brubaker, K.L. Precipitation, recycling, and land memory: An integrated analysis. *J. Hydrometeorol.* **2009**, *10*, 278–288. [CrossRef]
59. Song, Y.; Wang, Z.; Qi, L.; Huang, A. Soil Moisture Memory and Its Effect on the Surface Water and Heat Fluxes on Seasonal and Interannual Time Scales. *J. Geophys. Res. Atmos.* **2019**, *124*, 10730–10741. [CrossRef]
60. Donat, M.G.; Lowry, A.L.; Alexander, L.V.; O'Gorman, P.A.; Maher, N. More extreme precipitation in the world's dry and wet regions. *Nat. Clim. Chang.* **2016**, *6*, 508–513. [CrossRef]